Fermilab Library
0 1160 0052846 7

July 4, 1994
INFN PI/AE 94/08

Laboratory tests of a high resolution scintillating fibre hodoscope

A. Cardini*, V. Cavasinni*, B. Di Girolamo*, V. Flaminio*, A.M. Gorin†, P.V. Khaustov‡, D. Rizzi*

Submitted to Nuclear Instruments and Methods in Physics Research

*Dipartimento di Fisica, Università di Pisa and Istituto Nazionale di Fisica Nucleare, Sezione di Pisa, Italy
†IHEP, Protvino, Russian Federation
‡Budker Institute of Nuclear Physics, Novosibirsk, Russian Federation

Laboratory tests of a high resolution scintillating fibre hodoscope

A. Cardini[*] V. Cavasinni[*] B. Di Girolamo[*] V. Flaminio[*]
A.M. Gorin[†] P.V. Khaustov[‡] D. Rizzi[*]

July 5, 1994

Abstract

We report on the performance of a scintillating fibre tracking detector, read out by a microchannel-plate position-sensitive photomultiplier. Characteristics of the detector seem promising for possible use at the future high luminosity colliders.

Submitted to Nuclear Instruments and Methods in Physics Research

[*]Dipartimento di Fisica, Università di Pisa and Istituto Nazionale di Fisica Nucleare, Sezione di Pisa, Italy

[†]IHEP, Protvino, Russian Federation

[‡]Budker Institute of Nuclear Physics, Novosibirsk, Russian Federation

1 Introduction

Extensive studies of scintillating fibre trackers for future high luminosity colliders have been carried out over the last years [1, 2, 3]. The most demanding requirement of a fibre detector is the readout system that should be at the same time efficient, compact, radiation resistant, fast and not too expensive. While an optimal solution has not been found yet, several solutions have been proposed: solid state photomultipliers (VLPC) [2], position-sensitive photomultipliers (PSPM) [4, 5, 6], delay tubes [7].

We have performed tests on a scintillating-fibre hodoscope read out by a 100-channel microchannel-plate PSPM. The hodoscope consists of 4 layers of 1.5 m long scintillating fibres, 0.5 mm in diameter. The foreseen space accuracy and granularity of the device was thus adequate for a possible use as central tracker in LHC experiments. The readout was performed through a FEU-2MKP-100 microchannel plate PSPM (MCPM), manufactured by Research Centre GEOSPHAERA, Moscow. The limiting factor in this simple scheme is the rather low quantum efficiency of the photocathode, hardly adequate for reliable detection of typical signals from the fibres used (10-20 photons)

Special care in this test was dedicated to investigate the track reconstruction capability of this detector which, due to the low efficiency of the photomultiplier, would require a large number of layers of fibres, thus limiting the development of this simple and attractive option.

In addition to the tests carried out with the hodoscope, extensive measurements have been performed on a large variety of types of single fibres.

2 Hodoscope and readout

2.1 The MCPM

The SciFi hodoscope is readout by a position-sensitive microchannel-plate photomultiplier (MCPM) with a fibre-optic window. The MCPM has a multi-alkali Sb-K-Na-Cs photocathode 25 mm in diameter, having a maximum quantum efficiency of about 5% in the green region. This device is a prototype and this low quantum efficiency may be increased in the future.

Two microchannel plates (MCPs) are used for amplification (fig. 1,2). The anode consists of 100 independent square shaped charge collecting pads with a gap of 0.2 mm between each other, arranged in a square matrix of 10 $\times$ 10 elements. Each anode element measures $1.5 \times 1.5\ mm^2$. Due to the microchannel plate multiplication system the electron avalanche is well contained within the size of one element, and

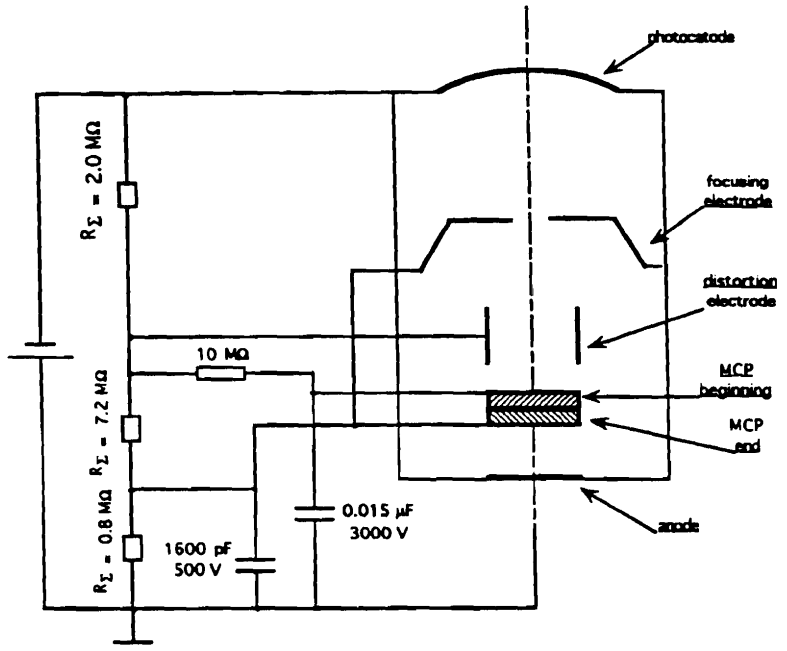

Figure 1: Schematic view of the MCPM and voltage divider circuit.

the crosstalk is lower (see section 2.2) than in case of other PSPM, like e.g. the Philips PSPM, which has a foil-dynode structure.

An amplification circuit was used to read out each output channel. The MCPM output pins were divided in four quadrants and for each quadrant a card containing 25 amplifiers was used. Harris HA-2540 operational amplifiers were used in a non-inverting configuration (fig. 3). These operational amplifiers were chosen because of their wide gain-bandwidth product (400 MHz) and very high slew rate (400 V/μs). The chosen gain of 100 implies a rise time of 87.5 ns. To decrease the heating in the PM housing (an alluminium box), due to the power dissipation of the circuit, an amplifier supply voltage of ± 8 V was chosen.

The total system (PM + Amps + cables) delay was 120 nsec, an additional 10 nsec delay was due to the cables used to connect the cable panel (where all the amplifiers are connected through 15 m long cables) to the ADCs.

We determined the position of each channel on the input MCPM window by scanning its surface with a fibre illuminated by a UV lamp, looking for positions for each channel which gave maximum signal and minimal cross-talk. Subsequently a specially designed mask, having one hundred, 0.5 mm diameter holes at the locations

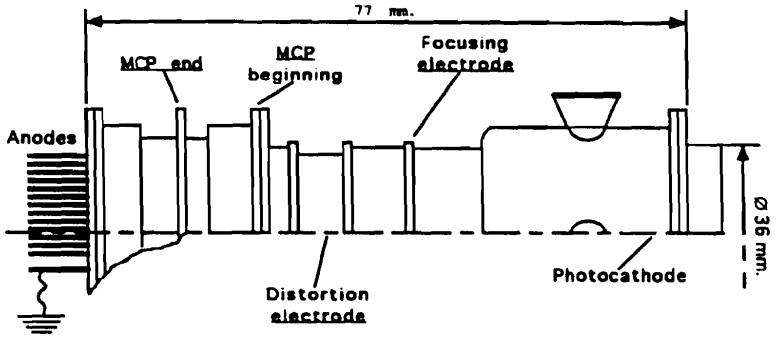

Figure 2: Mechanical structure of the MCPM.

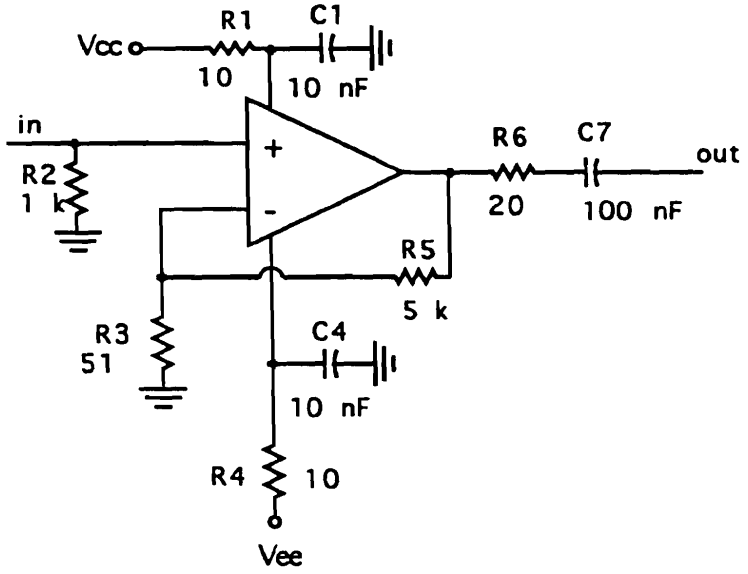

Figure 3: Amplification circuit for one MCPM channel.

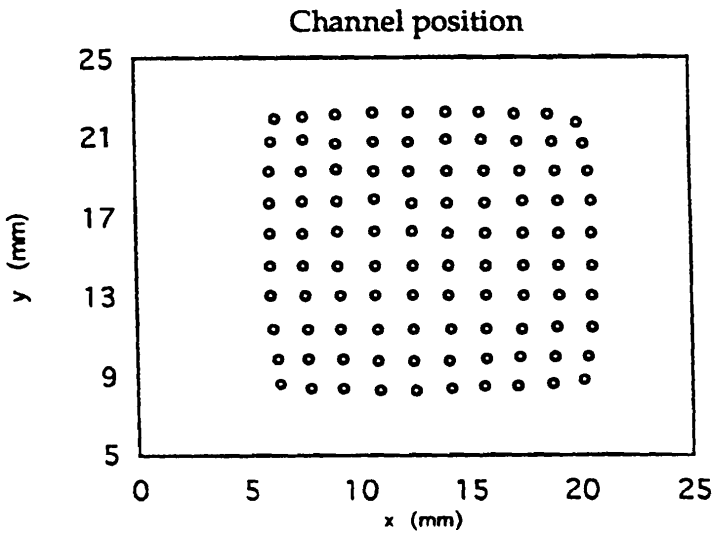

Figure 4: Channels coordinates on the photocathode.

of the channels on the MCPM input window was built. The non-ideal internal electrostatic photoelectron focusing of the MCPM causes a distortion of the image: a projection of the square anode matrix elements converts into a barrel-like shape on the photocathode surface (fig. 4).

The main characteristics of the MCPM are:

- Gain $= 3 \times 10^5$ at 2600 V;
- Channel size $\simeq 1.5$ mm at the photocathode surface;
- Pulse rise time $= 2$ ns.

Anode signals are amplified and connected to eight LeCroy 2249A 12 channels ADC modules. Channels corresponding to the four corners of the PM were not read out.

The trigger provides a 200 ns gate to each ADC module (fig. 5).

In this way, each event consists of an array of 96 ADC outputs, each representing the charge collected by the corresponding anode element. This information may then be used to find those fibres that have been hit and for two dimensional track reconstruction.

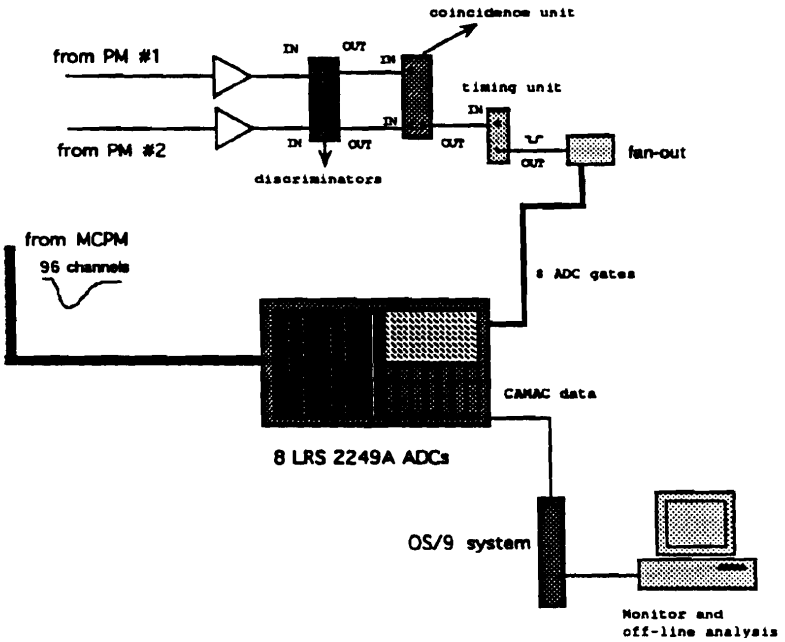

Figure 5: Schematic view of the readout electronics. PMs 1 and 2 are used for triggering purpose.

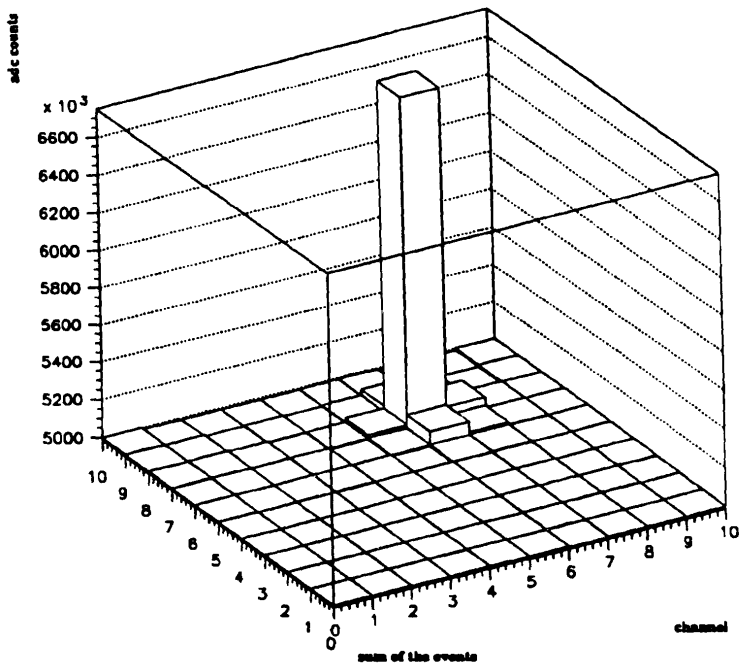

Figure 6: Lego plot representing the photocatode surface with pulse height of the channels. One channel is illuminated.

2.2 Cross-talk of the MCPM

Measurements of several characteristics of the PSPM were done; one of the most significant is the evaluation of the internal cross-talk of the device.

We measured the cross-talk using clear fibres (1 mm in diameter) illuminated by a light emitting diode (LED) coupled to different MCPM channels. Thanks to the fibre-optic window the optical cross-talk is strongly reduced.

After a dedicated pedestal run, we took data illuminating either a single channel or several channels. In single fibre measurements we darkened all fibres, except one, by a black film on the fibre mask. Fig. 6 shows a lego plot of the 96 ADC channels content, accumulated during a run. Only one fibre was illuminated. The small signals visible on the adjacent channels may be explained by the angular divergence of the light output from a fibre, combined with the small gap between fibre end and MCPM surface, introduced by the black film used to darken the other fibres.

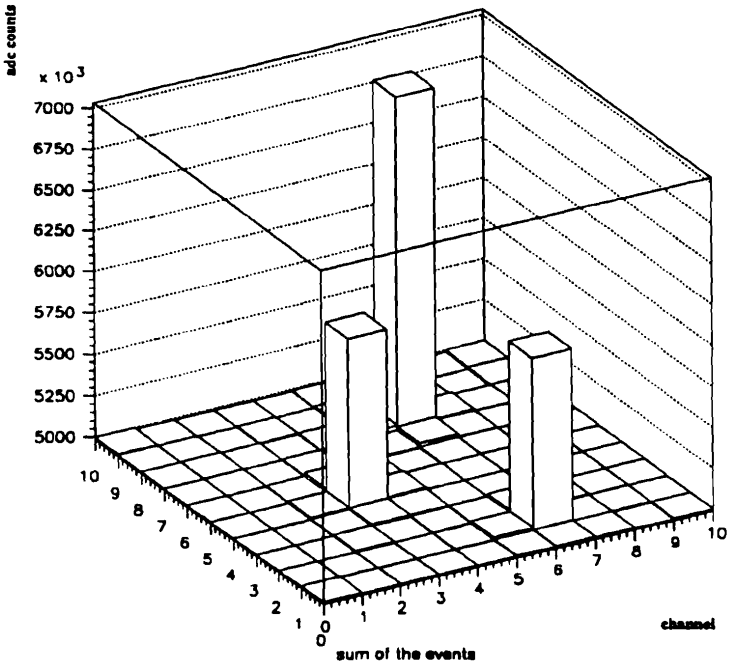

Figure 7: Lego plot representing the photocatode surface with pulse height of the channels. Three channels are illuminated.

Removing the black film the coupling improved and the result was good as shown in fig. 7; the different heights for the different three channels illuminated may be mainly due to a different quality of fibre end surfaces.

If we define the cross-talk as the ratio between the highest content of the adjacent channel and the content of the illuminated channel, we can set an upper limit of 1.5 % on the cross-talk between channels.

2.3 The hodoscope

The hodoscope was built by superimposing scintillating fibres ribbons 1.5 m long manufactured by Kuraray [8]. These ribbons were arranged in four layers, each consisting of 25 fibres.

The fibre hodoscope thus consisted of four layers, each having 25 fibres, staggered by half a fibre diameter (figures 8 and 9). The fibres at one end of the hodoscope

were positioned on the MCPM photocathode using the specially designed mask described above. Each fibre was glued, using a fast epoxy, in the corresponding hole. The opposite side of the mask was then polished. The mask was then fixed in a special holder and pressed against the MCPM window, allowing a good optical contact. The holder position can be adjusted by two orthogonal micrometer screws, allowing a high precision positioning along the MCPM input window.

2.4 Selection of the fibre type to be used for the hodoscope

A set-up for the measurement of the characteristics of the fibres to be used has been built in our laboratory. The early results obtained have been given in [3]. Since the MCPM has a peak quantum efficiency in the green region, green fibres have been chosen for our test. The best commercially available fibres from Kuraray [8] that we tested were the following:

1. single cladding, 0.5 mm in diameter;
2. single cladding, 0.835 mm in diameter;
3. double cladding, 0.5 mm in diameter;
4. double cladding, 0.835 mm in diameter;

All fibres are doped with 3HF (concentration of 1500 ppm), a scintillator with emission peak at $\lambda_{peak} = 530$ nm. The single cladding fibres have a PMMA cladding of 1.49 refraction index, surrounding the polystyrene fibre core of 1.58 refraction index. The double cladding fibres have two kinds of cladding materials: fluorinated polymethacrylate of 1.42 refraction index, surrounding the PMMA cladding and the polystyrene core.

Prior to the test with the hodoscope we performed tests on individual fibres to investigate their characteristics. Table 1 summarizes the results obtained. Here we quote the attenuation length (l_{att}), the number of photoelectrons at 0 cm (N_0) and the number of photoelectron at 50 cm (N_{pe} (50 cm)). The methods used are discussed in [3]. It has to be noted that these tests were performed with Hamamatsu R1635-02 photomultipliers with a larger efficiency ($\sim$ 12 %) at 530 nm than the MCPM used in the tests of the hodoscope.

Several different MCPM channels were tested, using both single and double cladding individual fibres and a ^{90}Sr source, to check the response uniformity in different regions of the photocathode. No significant differences in the response between individual MCPM channels were observed.

Fibre type	l_{att} (cm)	N_0 p.e.	$N_{p.e.}(50\ cm)$ p.e.
$SC3HF$ 500 μm	520	1.07	0.97
$DC3HF$ 500 μm	452	1.96	1.74
$SC3HF$ 835 μm	295	1.81	1.54
$DC3HF$ 835 μm	433	2.49	2.13

Table 1: Fibre characteristics

A charge spectrum of a Kuraray double cladding 0.5 mm fibre readout by the MCPM was taken and analyzed. The average number of photoelectrons found is $N_0 = 1.1$ p.e., thus we expect a 33 % probability for 0 photoelectrons. This implies that the single fibre detection efficiency, when a charged particle crosses it, is less than 67 %. Instead, in the case of single cladding fibres, like the ones used to build our final hodoscope, the average number of photoelectrons is only 0.6, yielding a single fibre efficiency smaller than 45 %.

The quoted efficiency represents an upper limit to the real efficiency in the fibre hodoscope because the 1 p.e. peak and the pedestal are not clearly separated (figure 10) and the threshold had to be adjusted to reach a compromise between a reasonable noise and maximum efficiency.

3 Tests of hodoscope performance in track detection of electrons from a ^{90}Sr source

3.1 Experimental setup

We used ^{90}Sr as a source of energetic electrons (maximum energy of 2.2 MeV). A minimum ionizing particle deposits about 0.3 MeV when crossing the hodoscope at 90°. Moreover, multiple scattering of low energy electrons produces large deviations from a straight line.

The radioactive source was placed above the hodoscope at a distance of 50 cm from the MCPM input window. The signals from HAMAMATSU R1635-02 photomultipliers, which in the following are referred to as PM1 and PM2, were used for triggering.

Two types of trigger were tried. In trigger #1 (fig. 8), a small scintillation

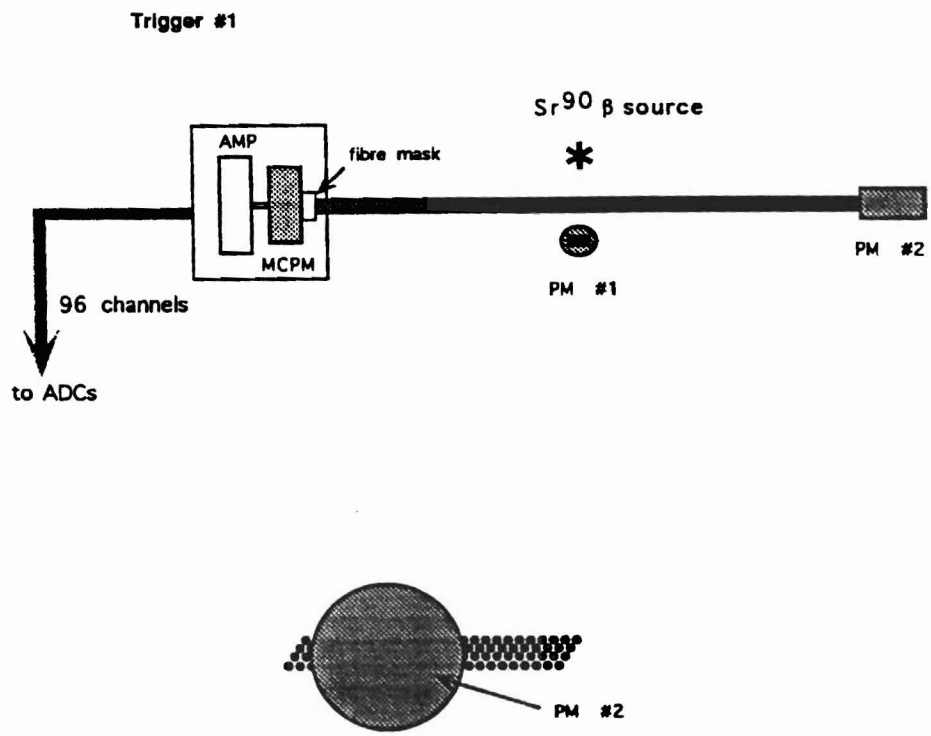

Figure 8: Schematic view of the setup using trigger #1. Top: side view; bottom: view from the end of the ribbon.

counter ($0.3 \times 13 \times 20\ mm^3$) viewed by PM1 was placed right under the hodoscope and the source, and the other PM2 viewed the fibres of the hodoscope itself from the end opposite to the one where the MCPM was positioned. The diameter of the photomultiplier input window is smaller than the hodoscope width, thus allowing to move the PM2 along the width of the ribbon and thus to examine the response of different sections of the hodoscope.

For trigger #2 we required the coincidence of signals from two 1 mm diameter scintillating fibres, placed one above the other, under the hodoscope and the source (fig. 9). This trigger is not affected by any bias, unlike the first one. Here also, as for trigger #1, we can move the trigger fibres across the hodoscope, allowing the measurement of the response to electrons of different parts of the detector.

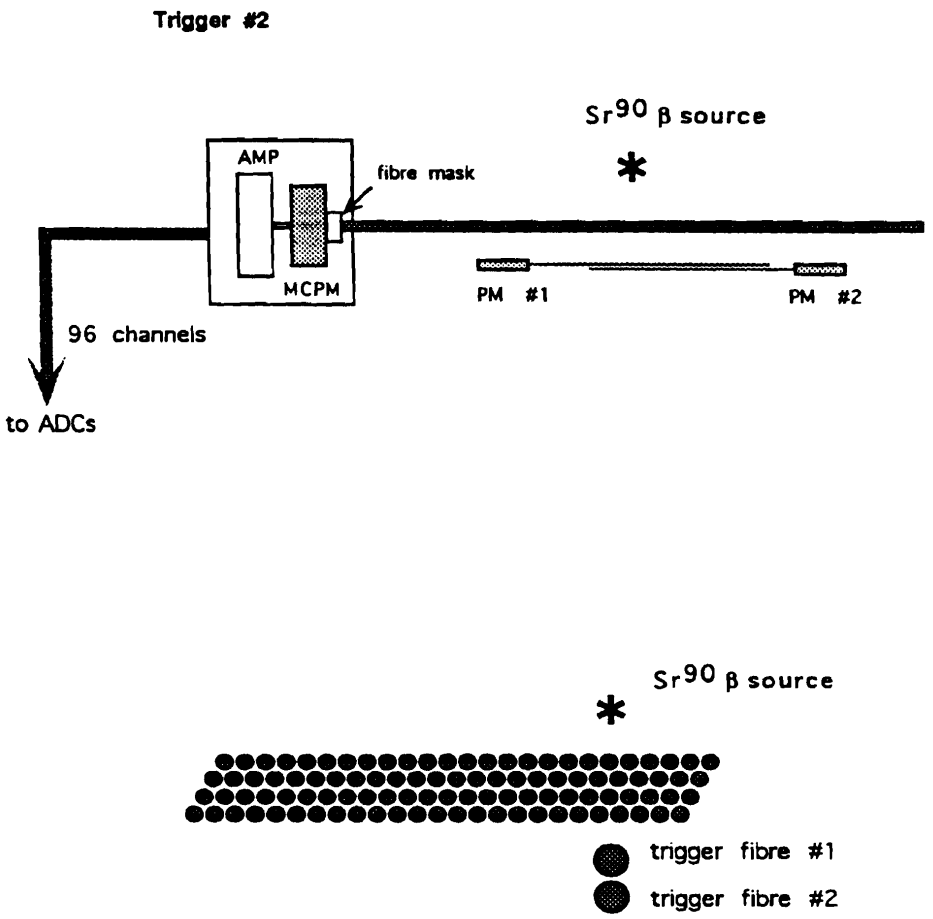

Figure 9: Schematic view of the setup using trigger #2. Top: side view; bottom: view from the end of the ribbon. The trigger fibre are 20 cm in length.

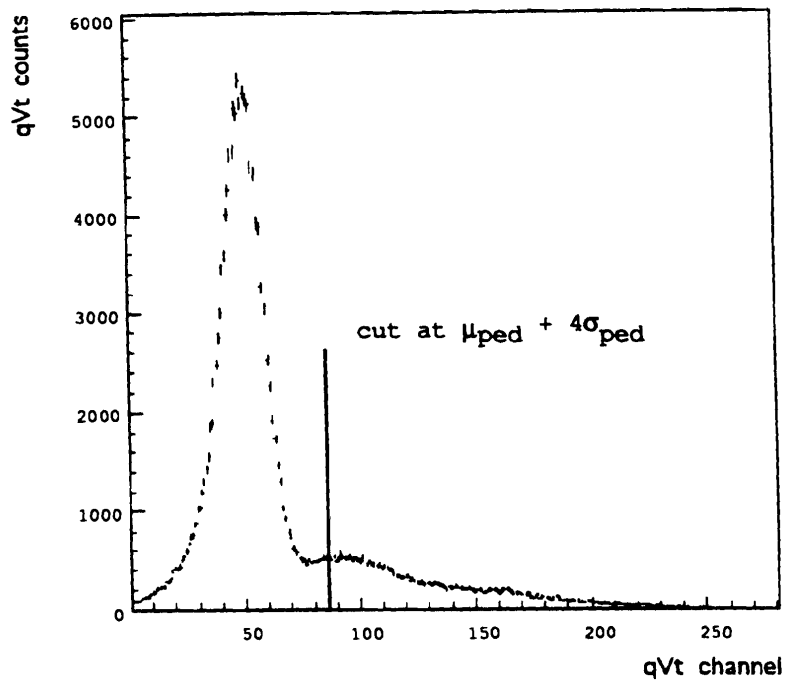

Figure 10: Charge spectrum obtained with the MCPM.

3.2 Analysis and results

For each of the two trigger types a data sample was taken and analyzed. All 96 ADC outputs (representing the signals from 96 hodoscope fibres) are written for each event. Pedestal averages and widths were extracted from a dedicated pedestal run using a pulser trigger. A fibre was taken to be hit if the corresponding ADC count was greater than the pedestal average plus 4 times the sigma of pedestal (fig. 10).

The pattern of hit fibres was then used to find tracks and to obtain the track parameters. The ratio between the number of tracks with hits in 3 or 4 layers (when the least-squares method is applicable) and the total number of events can be used to evaluate the hodoscope efficiency.

First, events with hits in only one or two layers were excluded. The remaining events, having hits in three or four layers were used in a standard track-searching procedure, based on the least-squares method. We assumed only one track to be present in a given event. The presence of two or more hits on a given layer is assumed to be due to:

- optical cross-talk;
- cross-talk inside the MCPM;
- noise.

Only one hit at a time from a given layer is thus used for the fit. All possible combinations of 3 hits in 3 different layers were tried for a straight line fit. The one having the lowest residual sum of squares was accepted. Parameters of the straight line fitting this hit combination and those of hit pattern are kept for further analysis. These parameters include: reconstructed track parameters, number of hits, number of layers containing hits, residual sum of squares (indicating the goodness of fit).

The reconstructed tracks generally do not have a very good residuals due to the large multiple scattering of electrons from the ^{90}Sr source and to deviations of fibre positions from the ideal ones. For this reason, no tight cut on the sum of squares was applied.

The result obtained for the track position (defined by the coordinate of the fitted straight line, at the location of the top layer, in units of fibre number) is shown in fig. 11.

As this shows, the track position moves when the trigger counter is moved in a direction perpendicular to the ribbon. The width of the distribution is consistent with the size of the trigger counters. The result obtained proves the reliability of our track reconstruction algorithm and shows that our data sample is not contaminated by large noise and crosstalk effects. Typical examples of tracks are shown in fig. 12 .

The ratio between the number of tracks having hits in three or four layers and the total number of events is found to be 15 % and 10 % for trigger #1 and #2 respectively. This yields single fibre efficiencies of 37 % and 32 %, in rough agreement with measurements on individual fibres. The similarity of these efficiencies shows that indeed trigger #1 is not affected by a large bias.

The low efficiency found is the result of the small quantum efficiency of the photocathode ($\sim$ 5 %) and the inherently low signal coming from the scintillating fibre. The use of double-cladding fibres, which have better light trapping properties (about a factor 2), and a better PM with 20 % quantum efficiency ($\sim$4 p.e. for a fibre in such conditions), would yield a hodoscope efficiency (defined as the ratio of events with hits in three or four layers to the total number of events) better than 99 %.

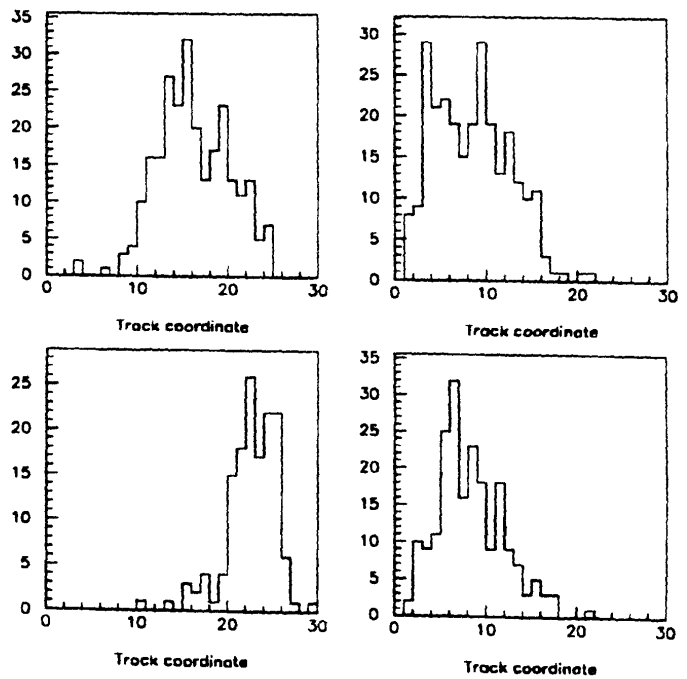

Figure 11: Track coordinate in terms of the fibre number for trigger #1 (above) and trigger #2 (below). Moving the trigger counter position (left and right) the track position moves.

Figure 12: Typical hit patterns with fitted straight line shown.

4 Conclusion

We performed a first test with a fibre hodoscope read by the MCPM. The efficiency for track reconstruction was low, due to intrinsic limitations of the signal from scintillating fibres and the low quantum efficiency of the MCPM photocathode.

Further optimization of our setup is possible (i.e. fibres with double cladding or capillaries filled with liquid scintillators [9], photomultiplier with higher quantum efficiency photocathode), but we estimate that major improvements will only be possible through the use of other types of photodetectors, having a higher quantum efficiency.

5 Acknowledgments

We wish to thank the director and technical staff of the INFN laboratory in Pisa and of the IHEP laboratory for their support. In particular we wish to thank Prof. G.M. Pierazzini, Mr. Bosi, Mr. E. Pucciarelli, Mr. R. Ruberti. Thanks are also due to Dr. N. Del Prete, Dr. E. Iacopini, Dr. Autiero for their help in early stages of these tests. We wish to thank as well our collaborators in the RD17 experiment and in particular Drs. K. Kuroda and A. Penzo for useful discussions.

References

[1] S.V. Golovkin et al., Nucl. Instr. and Meth. A305 (1991) 385.

[2] M. Atac et al., Nucl. Instr. and Meth. A314 (1992) 56.

[3] D. Autiero et al., Nucl. Instr. and Meth. A336 (1993) 521.

[4] J. Bähr et al., Nucl. Instr. and Meth. A324 (1993) 145.

[5] K. Kuroda et al., Nucl. Instr. and Meth. A300 (1991) 259.

[6] S. Majewski et al., Nucl. Instr. and Meth. A323 (1992) 489.

[7] T. Gys et al., Contrib. to ECFA Large Hadron Collider workshop, Aachen, FR Germany, 4-9 Oct 1990, CERN 90-10 vol. 3, 261.

[8] Kuraray Co., Ltd., Methacrylic Resin Division, Hatchobory 2-Chome, Chuo-ku, Tokyo 104, Japan.

[9] A. Cardini et al., INFN PI/AE/19/1993 to be published in Nucl. Instr. and Meth.